Cell Tissue Res (2013) 354:771–781
DOI 10.1007/s00441-013-1697-4

REGULAR ARTICLE

High-fat diet alters protein composition of detergent-resistant membrane microdomains

Elena Uyy · Luminita Ivan · Raluca Maria Boteanu · Viorel Iulian Suica · Felicia Antohe

Received: 29 April 2013 / Accepted: 3 July 2013 / Published online: 31 August 2013

Abstract A high-lipid diet is one of the main risk factors in atherosclerosis and can induce changes in the composition of plasma membrane microdomains. In response, important functions such as vesicle trafficking, protein docking, signaling and receptor recognition are significantly altered. In particular, interactions of heat-shock proteins (Hsps), acting as danger signals, with components of the membrane microdomains can influence signaling pathways and the inflammatory response of cells. Our study focuses on the composition of detergent-resistant membrane (DRM) isolated from ApoE−/− mice fed a standard or high-fat diet with and without fluvastatin treatment versus appropriate controls. Biochemical studies, immunoblotting and liquid chromatography mass spectrometric analysis were performed to investigate whether the structural components (such as caveolin and cavin) of the detergent-resistant microdomains were correlated with the expression and secretion of stress-inducible Hsps (Hsp70 and Hsp90) and AKT phosphorylation in experimental atherosclerosis. ApoE-/− mice challenged with a high-fat diet developed extensive atherosclerotic plaques in lesion-prone areas. DRM harvested from hyperlipidemic animals showed a modified biochemical composition with cholesterol, glycerolipids, caveolin-1 and phospho-AKT being up-regulated, whereas cavin-1 and dynamin were down-regulated. The data also demonstrated the co-fractionation of Hsps with caveolin-1 in isolated DRM, expression being positively correlated with their secretion into blood serum. Statin therapy significantly attenuated the processes induced by the development of atherosclerosis in ApoE−/− mice under a high-fat diet. Thus, high-lipid stress induces profound changes in DRM biochemistry and modifies the cellular response, supporting the systemic inflammatory onset of atherosclerosis.

Keywords Hyperlipidemia · DRM proteomics · Heat-shock proteins · Caveolin-1 · Cavin-1

Introduction

Atherosclerosis is now considered a multifactor disease characterized by inflammatory pathways and by specific cellular and humoral immune reactions. Data accumulated in the last few years support the hypothesis that the term “vulnerable patient” might be appropriate to identify subjects with a high potential of developing cardiovascular events with a fatal ending (Naghavi et al. 2003).

A large variety of signaling macromolecules are located in specialized membrane microdomains enriched in cholesterol and sphingolipids, are known as lipid rafts. Caveolae are specialized lipid rafts that form flask-shaped invaginations of the plasma membrane stabilized by the interaction between coat proteins (caveolins; Kurzchalia and Parton 1996; Drab et al. 2001) and adapter proteins (cavins). Membrane microdomains are involved in cell signaling and the transport of macromolecules and have been shown

E. Uyy and L. Ivan contributed equally to this work.

This work was supported by POSDRU project no. [89/1.5/S/60746] and the Romanian Academy and Ministry of Education and Research grant CNCSIS-UEFISCSU [PN-II-PCCA-2011-3 nos. 135 and 153/2012]. The mass spectrometry experiments were performed during a training internship at the Luxembourg Clinical Proteomics Department, Centre de Recherché Public de la Santé, Luxembourg, funded by project [346 PN-II-ID-PCE, code no. 159] CNCSIS-UEFISCSU and CARDIOPRO project ID:143, ERDF co-financed investment in RTDI for Competitiveness.

Electronic supplementary material The online version of this article (doi:10.1007/s00441-013-1697-4) contains supplementary material, which is available to authorized users.

E. Uyy · L. Ivan · R. M. Boteanu · V. I. Suica · F. Antohe (✉)
Institute of Cellular Biology and Pathology “Nicolae Simionescu”, 8 BP Hasdeu Street, PO Box 35-14, 050568 Bucharest, Romania
e-mail: felicia.antohe@icbp.ro

to regulate vascular reactivity and blood pressure (Durante et al. 1997). Caveolae have been implicated in chronic inflammatory conditions and other pathologies including atherosclerosis, pulmonary dysfunctions, inflammatory bowel disease, muscular dystrophy and generalized dyslipidemia (Simionescu and Simionescu 1991; Simionescu and Antohe 2006; Chidlow and Sessa 2010; Uyy et al. 2010). Recently, published data have shown that the function of caveolae can be modulated by nutrition, such as dietary lipids and plant-derived polyphenols, with profound changes in the caveolae-associated signaling pathways (Majkova et al. 2010). Because of their specific composition and detergent resistance, enriched fractions of these structures, called detergent-resistant membranes (DRMs) can be easily isolated (Sargiacomo et al. 1993).

Several antigens have been implicated in immune-mediated processes related to atherosclerotic plaques (Wick et al. 2004) and in particular, a role has been hypothesized for several heat-shock proteins (Hsps; Pockley and Frostegard 2005; Wick 2006). In addition to being present in cells under physiological conditions, Hsp expression increases in response to many environmental stresses, including oxidative stress, chemicals, viruses and ischemia-reperfusion injury (Mehta et al. 2005). Published data support the hypothesis that intracellular Hsps have cytoprotective functions, whereas extracellular located or membrane-bound Hsps mediate immunological functions (Tsan and Gao 2004). However, the mechanism by which Hsps are released into the extracellular space or secreted into the plasma and the specific role played in signal transduction have not yet been identified. In atherosclerotic lesions, human Hsps together with bacterial pathogen appear to stimulate an immune response leading to the development and progression of atherosclerosis (Pockley 2002; Businaro et al. 2009). Hsps are known to be associated with a number of signaling molecules, including v-Src, Raf1, AKT and steroid receptors, suggesting an important role for these proteins in signal transduction (Nollen and Morimoto 2002; Pratt and Toft 2003). One of the important areas of current research is to investigate the role of Hsps in atherosclerosis. Whether Hsps are protective or destructive for the organism, with the role of Hsps in atherosclerosis most probably being multifaceted, remains unclear.

ApoE-deficient (ApoE−/−) mice challenged with a high-fat diet developed extensive atherosclerotic plaques in the lesion-prone area with similar patterns to those in human patients. Accumulated results support the concept that the progression of the disease is closely associated with long-term systemic vascular dysfunction that leads, in the final stages, to plaque rupture and mortality. Given the widespread acceptance of the ApoE−/− mouse (Zhang et al. 1992; Nakashima et al. 1994; Smith and Breslow 1997; Kanwar et al. 2001) as a model of human atherosclerosis, the present study aims to determine whether atherogenesis in ApoE−/− mice correlates with the modified composition of isolated DRM and secretion of Hsps (Hsp70 and Hsp90). The effect of lipid-lowering therapy with statin, which inhibits 3-hydroxy-3 methylglutaryl coenzyme A reductase, has been used to evaluate the potential of the drug to prevent the progression of atherosclerotic disease.

The DRM content of the angiotensin-converting enzyme (ACE) as a key enzyme in cardiovascular pathophysiology (Bernstein et al. 2005) has been evaluated. ACE is critically involved in endothelial homeostasis by controlling the circulating levels of bradykinin and angiotensin II and thereby affects vascular development, tone and permeability, particularly in the lung, the organ with the highest level of endothelial cell ACE expression. ACE activity in lung endothelial cells is also a sensitive marker of endothelial dysfunction, including lung vascular injury (Muzykantov and Danilov 1991; Orfanos et al. 2000).

Since diet-induced hyperlipidemia might affect the composition of macromolecules located in lipid raft/caveolae, a platform for pro-inflammatory signaling associated with vascular diseases such as atherosclerosis, we designed experiments on DRM isolated from ApoE−/− mice exposed to a standard or hyperlipidemic diet with and without fluvastatin treatment versus control C57 Black mice. Biochemical studies, immunoblotting and high-sensitivity liquid chromatography mass spectrometric (LC-MS/MS) analysis were performed to investigate: (1) the total protein, glycerolipids, cholesterol concentration and ACE activity in DRM after a high-fat diet; (2) the caveolin-1, cavin-1 (PTRF [polymerase I and transcript-release factor]), filamin A and dynamin expression in microvascular DRM isolated from the lung tissue of ApoE−/− mice versus appropriate controls; (3) whether the expression and secretion of stress-inducible forms of Hsps (Hsp70 and Hsp90) were correlated with the caveolin intracellular distribution and activated AKT in experimental atherosclerosis; and (4) the effect of fluvastatin on the expression of Hsps and other DRM-located proteins in ApoE−/− mice.

Materials and methods

Antibodies and reagents

Antibodies and their sources were as follows: mouse anti-caveolin-1 monoclonal antibody clone C060 (from BD Transduction Laboratories, Lexington, Ky., USA); primary capture antibodies against Hsps (Hsp70 clone BRM-22 and Hsp90 clone AC-16) and anti-mouse and anti-rabbit IgG peroxidase conjugate (from Sigma, Mo., USA); biotinylated monoclonal antibodies against Hsps (Hsp70 clone 5A5 and Hsp90 clone AC88), AKT1, phosphorylated AKT1 (pAKT1), PTRF and β-actin clone AC-15 (from Abcam, Cambridge, UK). The enhanced chemiluminescence (ECL)

plus Western blotting detection reagent kit was supplied by GE Healthcare (Little Chalfont, UK). All other reagents were purchased from BIO-RAD or Sigma, except when otherwise specified.

Animals

Healthy male 8-week-old ApoE−/− (n=20) and wild–type C57 BL (n=10) mice, selected to have a body weight of 20±2 g, were divided into three experimental groups of 10 animals each. The control group (WT) was represented by wild–type C57 BL mice. The atherosclerotic group (A) of ApoE−/− mice was fed for 4 weeks with a hyperlipidemic diet (standard diet supplemented with 1 % cholesterol and 15 % butter). In parallel, another atherosclerotic group (At) was fed the same hyperlipidemic diet and after 4 weeks received fluvastatin (10 mg/kg/day) by oral gavages for other 2 weeks (Nakamura et al. 2009).

The animals were evaluated for general physical aspects and plasma biochemical values of cholesterol and triglycerides; when plasma cholesterol reached the pathological level of 300–470 mg/dl, the animals were anesthetized and then killed and their blood, hearts, aortas and lungs were harvested and kept frozen at −80 °C until use. During the experiment, animals had free access to fresh water. The experiments were conducted in accordance with the Principles of Laboratory Animal Care (NIH Publication no. 83–25, revised in 1985), regulations of the Ethics Committee of ICBP N. Simionescu and Romanian Law no. 471/2002.

Cryosections

Tissue fragments from the aortic arch and heart valve were collected from each experimental group and processed for microscopy. Aorta and cardiac valves were carefully excised and all segments were fixed in 4 % formaldehyde in phosphate-buffered saline (PBS) for 90 min at room temperature. The tissue fragments were then immersed in OCT embedding medium and flash-frozen in liquid nitrogen and cryosections were collected. The frozen sections were stained with Oil Red O (Mancini et al. 1995) and hematoxylin-eosin or Hoechst, mounted in 90 % glycerol in water and examined by fluorescent microscopy by using a Zeiss AXIOVert A1 microscope (Zeiss LD-Plan-Neofluar 20×/0.4 Ph2 Korr objective lens) at room temperature. Images were captured with a Zeiss AXIOcam MRc5 Camera by using ZEN imaging software. The post-processing of images was performed with Adobe PhotoshopCS5.

Enzyme-linked immunosorbent assay

Levels of Hsps (Hsp70 and Hsp90) in serum samples were detected in 96-well plates coated with 2 μg/ml anti-Hsps capture antibody diluted in coating buffer, overnight at 4 °C. The following day, the wells were blocked with 1 % bovine serum albumin (BSA) in PBS (200 μl/well) for 2 h at room temperature. Before the addition of the samples, the plates were washed three times with washing buffer (PBS containing 0.05 % Tween 20). Standard and serum samples (diluted 1:2 in PBS) were added to each well (100 μl/well) in duplicate. Following overnight incubation, the plates were washed (three times) and 100 μl biotinylated anti-Hsps antibody (1 μg/ml diluted in 1 % BSA in PBS) was added and incubated in the plates for 2 h. Afterwards, 100 μl/well streptavidin-horseradish peroxidase (HRP) was added and incubated for 1 h at room temperature. After a washing step, 100 μl/well working substrate solutions (containing 0.1 M citric acid, 0.2 M disodium hydrogen phosphate, 0.08 % o-phenylenediamine and 0.01 % H_2O_2) were added and the plates were incubated for 15 min in the dark at room temperature. Finally, 8 M H_2SO_4 (25 μl/well) was added to stop the reaction. Absorbance was measured at 492 nm with a Multiskan MS 3.0 (Labsystems) micro-plate spectrophotometer.

Preparation of DRM

Lung tissue fragments (200 mg) were homogenized in 2 ml cold buffer with 1 % Triton X-100, adjusted to a final concentration of 40 % sucrose and bottom-loaded in an ultracentrifuge tube. DRM fractions were purified as previously described (Sargiacomo et al. 1993). A discontinuous gradient consisting of 30 % and 5 % sucrose was formed on top of the sample and the gradient was centrifuged for 18 h at 200,000 g. Buoyant lipid raft and caveolae material floated up to the 30 % to 5 % sucrose interface (DRM fractions 4 and 5), whereas the rest of the cellular material remained in the 40 % sucrose layer. The gradient was collected in aliquots of 1 ml starting from the top. For all fractions, protein, cholesterol and glycerolipid concentrations were determined by using the Precision Red protein assay (Cytoskeleton, Denver, Colo., USA), the cholesterol assay kit (CHOD-PAP method) and the triglycerides assay kit (GPO-PAP method; Dialab, Austria), respectively. ACE activity was quantified by using Hip-L-His-L-Leu substrate (Erman et al. 1993).

Immunoblot assay

Fractions 4 and 5 (enriched in cholesterol and protein) were pooled together and equal amounts of protein from each sample were loaded and run on 12.5 % sodium dodecyl sulfate/polyacrylamide gels. The separated proteins were then transferred to nitrocellulose membrane and analyzed by Western blot assay. The blots were blocked with 5 % BSA in TRIS-buffered saline (TBS) with 0.05 % Tween 20, pH 7.6 and exposed for 2 h to the primary anti-caveolin-1

and anti-PTRF antibodies in TBS with 1 % BSA followed by the appropriate IgG–HRP secondary antibodies for 1 h. The reaction product was detected with the Super signal chemiluminescence substrate and quantified by densitometry with computerized image analysis Scion Image software.

DRM preparation for mass spectrometric analysis

DRM fractions were diluted in MES-buffered saline and ultra-centrifuged for 4 h (100,000 *g*) and the resulting pellets were subsequently prepared for mass spectrometry analysis. The procedure included solubilization in 8 M urea and 1 % sodium deoxycolate denaturant buffer, purification (delipidation by using methanol/chloroform/water precipitation), reduction for 1 h at room temperature by using 20 mM dithiotreitol solution and alkylation of cysteine residues for 1 h 30 min at room temperature by using 80 mM iodoacetamide solution. Urea dilution was performed with ammonium bicarbonate (50 mM), which was also used to buffer the solution (pH ~8). Overnight proteolysis was performed at 37 °C by using sequencing-grade modified trypsin (Enzyme: Substrate=1:20; Promega, Madison, Wis., USA) under agitation. The resulting peptide solution was acidified with 1 % formic acid (pH ~3) and then desalting through solid-phase extraction of the peptides by using 100 mg sorbent Sep-Pak C18 cartridges (Waters, Milford, Mass., USA) was performed. Peptides were eluted with 50 % acetonitril, 0.1 % formic acid solution, dried by using the Concentrator Plus (Eppendorf) and suspended in 5 % acetonitril with 0.1 % formic acid solution.

Nano LC-MS/MS analysis

The peptide mixtures (0.5 μg) were separated by using the Ultimate 3000 RSLC nano system (Dionex, now part of Thermo Fisher Scientific, San Jose, Calif., USA). For each analysis, the sample was loaded into an Acclaim PepMap 2 cm×75 μm i.d., C18, 3 μm, 100 A, trap column (Dionex). The trap column was connected to the Acclaim PepMap RSLC 15 cm×75 μm i.d., C18, 2 μm, 100 A, analytical column (Dionex). The aqueous mobile phase was 0.1 % formic acid in high-pressure LC (HPLC) grade water (solvent A), whereas the organic mobile phase contained 0.1 % formic acid in HPLC grade acetonitril (solvent B). After 3 min of washing the trap column, peptides were eluted with a gradient of 2–35 % solvent B over 48 min at a flow rate of 300 nl/min. Dynamic nano-electrospray source housing was utilized with uncoated SilicaTips, 12 cm length, 360 μm outer diameter, 10 μm tip inner diameter. For the ionization process, 1,500 V liquid junction voltage and 250 °C capillary temperature were used. The mass spectrometer was operated in a top 6 data-dependent configuration at 60 k resolving power (at m/z=400) for a full scan with monoisotopic precursor selection enabled and mass correction by using lock mass, in the 300–2,000 m/z domain. The dynamic exclusion mode was enabled over a duration of 90 s, with an exclusion mass width relative to the precursor of ±7 ppm. The analyses were carried out with CID fragmentation mode. The instrument operating software was Xcalibur 2.1.0 QF03489 build 1140 and LTQ Orbitrap Velos MS 2.6.0 build 1050. The samples were injected in triplicate (see Electronic Supplementary Material, Table S1).

Protein database inference and label-free quantification

The identification process was performed by using Proteome Discoverer 1.3 (Thermo Fisher Scientific) and Scaffold 3.0 (Proteome Software, Portland, Ore., USA). Only one missed cleavage was allowed. A mouse database (UniProtKB/Swiss-Prot, build 28.11.2012) was used for the identification search. Moreover, Mascot Score (Matrix Science, London, UK; version 1.2.0.207) was cross-correlated with X!Tandem (The GPM, thegpm.org; version 2007.01.01.1) for better identification significance. Mascot and X!Tandem were searched with a fragment ion mass tolerance of 0.80 Da and a parent ion tolerance of 10.0 ppm. Oxidation of methionine and carbamidomethylation of the cysteine residues were specified in Mascot and X!Tandem as variable modifications. Peptide identifications were accepted if they could be established at greater than 95 % probability as specified by the Peptide Prophet algorithm (Keller et al. 2002). Protein identifications were accepted if they could be established at greater than 99 % probability and contained at least two identified peptides. Protein probabilities were assigned by the Protein Prophet algorithm (Nesvizhskii et al. 2003). Label-free relative quantification was performed by using the spectral counting method within Scaffold (version Scaffold_3.0.9.1, Proteome Software).

Spectral counting is an often-used label-free quantitative strategy in which the number of spectra matched to peptides from a protein is taken as a surrogate measure of protein abundance. Although conceptually simple, various studies have demonstrated that spectral counting can be as sensitive as ion peak intensities in terms of detection range, while retaining linearity (Ishihama et al. 2005; Fu et al. 2008). Scaffold calculates the spectrum count quantitative value by normalizing spectral counts across an experiment. The process of calculating normalized spectral counts is as follows: Scaffold takes the sum of all the un-weighted spectrum counts for each MS sample; these sums are then scaled so that they are all the same; Scaffold applies the scaling factor for each sample to each protein group and outputs a normalized quantitative value.

Statistical analysis

All results were expressed as means ± SEM. All statistical comparisons were performed by using a one-way analysis of variance test. A probability value of $P<0.05$ was considered statistically significant.

Results

Characterization of the experimental model

ApoE−/− mice from the A group received a hyperlipidemic diet in order to accelerate the development of atherosclerotic plaques. Whereas the body weight remained almost constant, the onset and development of hyperlipidemia was assessed by the significant increase of serum cholesterol and triglycerides concentrations under the hyperlipidemic diet when compared with the control (WT) group (Table 1). After receiving a standard diet, the control animals had a plasma cholesterol level of 65.6±1.7 mg/dl, whereas under a hyperlipidemic diet, the A group animals presented a significantly higher plasma cholesterol level of 472.5±79.9 mg/dl. Additionally, the triglyceride level was also increased to 130.8±39.6 mg/dl in the A group animals compared with 46.1±2.1 mg/dl in the control animals. Notably, the hyperlipidemic diet effect was significantly attenuated when the serum levels of cholesterol (100 mg/dl) and triglycerides (50.3 mg/dl) were evaluated after treating the At group animals with fluvastatin (Table 1).

All ApoE−/− mice challenged with the hyperlipidemic diet developed substantial atherosclerotic lesions in the proximal aorta and valves. Lipid deposits were detected on serial sections of heart valves by staining with the lipid-soluble dye Oil Red O, which stained hydrophobic lipids, including cholesterol esters (Fig. 1b, c, e, f). In contrast, none of the controls showed the development of typical atherosclerotic lesions (Fig. 1a, d). Lesion areas were characterized by a heterogeneous structure enriched in cells loaded with fat droplets intensely stained with Oil Red O and hematoxylin-eosin (Fig. 1b, c). The double-staining with Hoechst and Oil Red O clearly demonstrated the close association of lipid deposits with cellular structures of the plaques (Fig. 1e, f). Control mice showed no abnormalities in any of the stained sections examined, whereas ApoE−/− mice developed atherosclerotic plaques in several locations. Markedly, in correlation with the serum lipid detected (Table 1), statin therapy delayed the growth of atherosclerotic plaques, which were still present as fatty streaks in the tissue fragments harvested from group At animals (Fig. 1c, f).

Characterization of isolated DRM

DRMs were prepared from lung tissue, the organ with the largest surface of endothelial cells endowed with characteristic caveolae structures and often used as a source to isolate endothelium enriched samples. The maximum protein expression of caveolar marker caveolin-1 was found in fractions 4 and 5 of the Triton-X-100-resistant membrane extraction and in fractions 9–12 of non-raft origin in a similar pattern as previously reported (Razani and Lisanti 2001; data not shown). Fractions of raft origin were pooled together and further named DRMs.

ACE-assayed activity was found to be higher in DRM isolated from all animal groups (Fig. 2a). These increased values of ACE (marker of endothelial cell plasma membrane) activity showed the significant enrichment of our extract in endothelial cells plasma membranes. Notably, the ACE activity was even higher in groups A and At, suggesting the activation of endothelial cells under hyperlipidemic stress.

Protein, cholesterol and glycerolipids concentration increased in DRM in all experimental groups (Fig. 2b–d). The concentration of cholesterol in DRM was ~2 times

Table 1 Biochemical parameters of the atherosclerotic model. Characteristics of control (*WT*) and hyperlipidemic untreated (*A*) and statin-treated (*At*) animals. Assays of blood serum cholesterol, triglycerides, Hsp70, Hsp90 and measurements of body weight were performed for each group. Data are expressed as means ± SEM (*a.u.* arbitrary units)

Parameter measured	Experimental group		
	WT	A	At
Body weight (g)	20.2±0.7	20.6±0.5	20.3±0.4
Cholesterol (mg/dl)	65.6±1.7	472.5±79.9***	100.4±20.1***(vs. A)
Triglycerides (mg/dl)	46.1±2.1	130.8±39.6*	50.3±2.2
Hsp 70 (a.u.)	81.57±3.4	118.43±6.5***	79.43±3.9***(vs. A)
Hsp 90 (a.u.)	49.71±5.8	13.28±3.6*	36.28±8.5*(vs. A)

*$P<0.05$

***$P<0.001$

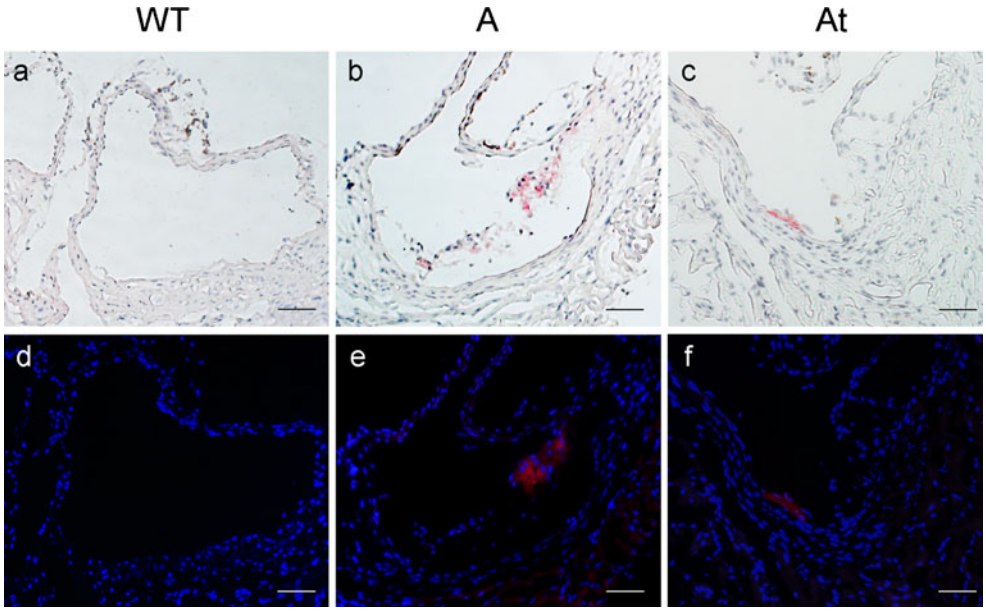

Fig. 1 Atherosclerotic plaques developed on cardiac valves. Cryosections of cardiac tissue harvested from wild-type (*WT*) control C57 Black (**a**, **d**) and hyperlipidemic untreated (*A*) and statin-treated (*At*) ApoE−/− mice (**b**, **e**, **c**, **f**). Hematoxylin-eosin and Oil Red O phase-contrast images (**a**, **b**, **c**) showing the lipid deposits in A (**b**) and At (**c**) groups. Fluorescence microscopy of similar sections double-stained with Hoechst and Oil Red O (**d**, **e**, **f**) demonstrated the presence of lipid-loaded cells within the atherosclerotic plaques in the A (**e**) and At (**f**) groups. Note the reduced atherosclerotic lesion under statin administration (**c**, **f**). *Bars* 200 μm

greater in both A and At animals than in WT controls. The mass spectrometry analysis also demonstrated different amounts of identified proteins in the three experimental groups, namely: 465±14 in WT, 477±6 in A and 456±18 in At. This variable protein composition and the increase in cholesterol and glycerolipids concentration in DRM isolated from animals receiving a high-fat diet (Fig. 2c, d) indicated the modified biochemical composition of the cell membrane. Elevated membrane contents in cholesterol and glycerolipids might significantly affect the plasma membrane fluidity and permeability in atherosclerosis and in tissues that do not usually develop atherosclerosic plaques.

Hyperlipidemia induces the up-regulation of caveolin-1 protein expression in DRM

We investigated whether the expression of caveolin-1 in DRM isolated from lung tissue could be influenced by a hyperlipidemic diet. Caveolin-1 was specifically detected by Western blot as a 22-kDa band in all experimental groups. The densitometry measurements of individual bands showed that caveolin-1 expression was 2.5-fold higher in the A group animals and 2.3-fold higher in the At group animals compared with probes from WT animals (Fig. 2e).

Expression of caveolin-1 was also evaluated by comparative spectral counting LC-MS/MS proteomics. The data showed that caveolin-1 was over-expressed in the DRM isolated from the A and At groups than in the WT group (Fig. 3a), which supported the immunoblotting detection results.

Extraction with Triton X-100 detergent followed by density gradient centrifugation generated a mixture of membranes from several organelles (Rizzo et al. 1998; Everson and Smart 2006) rich in cholesterol and sphingolipids but also in ACE, indicating the endothelial origin of the proteins concentrated in DRM. Increased expression of caveolin-1 protein induced by hyperlipidemia in DRM supported the hypothesis of the redistribution of caveolin-1 between the intracellular and plasma membranes, an event that might generate the over-expression of caveolin-1 in the isolated DRM.

Hyperlipidemia induces the down-regulation of PTRF protein expression in DRM

Because the presence of cavin-1 (PTRF) in membranes has an important role in caveolae formation at the plasma membrane level, PTRF protein expression was evaluated by Western blotting and mass spectrometry in DRM (Figs. 2e, 3a). As shown in Fig. 2e, the densitometry revealed that PTRF expression was significantly decreased in membrane-enriched fractions isolated from the A group and was not affected by the fluvastatin treatment when compared with the WT group.

This study showed a decrease in the protein expression of PTRF and an increased expression of caveolin-1 in DRM from hyperlipidemic (A) compared with control (WT) animals. The AKT1 level in group A was comparable with the basal level of AKT1 in the control group (WT), whereas a significant increase (2.4-fold) of pAKT was observed in the lung homogenate from the A group animals. The hyperlipidemic stress could be a determining factor for increased phosphorylation of AKT1 at Thr^{308}. Interestingly the pAKT level was significantly reduced (2.5-fold) by the fluvastatin treatment (Fig. 2f).

As PTRF selectively associates with mature caveolae at the plasma membrane but not with Golgi-localized caveolin

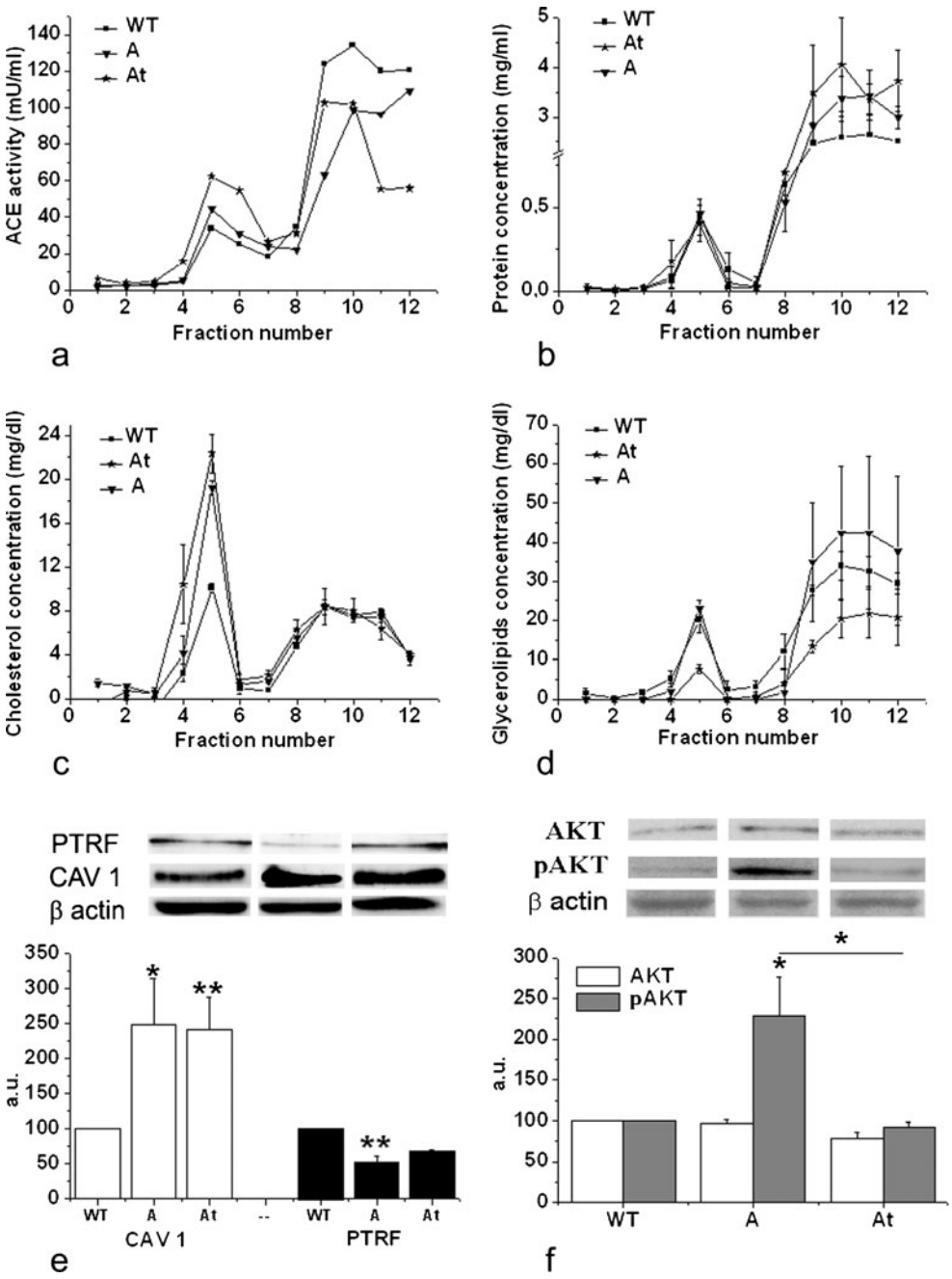

Fig. 2 Characterization of detergent-resistant membrane (DRM). Lung tissue from hyperlipidemic animal models and their controls (*WT* wild-types, *A* hyperlipidemic untreated animals, *At* statin-treated animals) was homogenized in buffer containing 1 % Triton X-100. The mixture was overlaid on a discontinuous sucrose gradient and subjected to ultracentrifugation to obtain DRM (fractions 4 and 5). Angiotensin-converting enzyme (*ACE*) activity (**a**), protein (**b**), cholesterol (**c**) and glycerolipid (**d**) concentrations were detected in all 12 fractions collected. Protein expression of caveolin-1 (*CAV1*) and cavin-1 (*PTRF*, polymerase I and transcript-release factor) was identified in DRM (**e**) and protein expression of AKT1 and phosphorylated AKT1 (*pAKT1*) was assayed (**f**) in the cytosolic fractions 9–12 by Western blotting. The protein expression of caveolin-1, PTRF, AKT1 and pAKT1 was reported in comparison with β actin, which was arbitrarily assigned to 100 in the wild-type (*WT*) case (*a.u.* arbitrary units). The experiment was repeated three times. Data are expressed as means ± SEM. **P*<0.05, ***P*<0.01 respectively

(Hill et al. 2008; Nabi 2009), our experimental data support the hypothesis that the lower protein expression of PTRF leads to a reduction in the number of caveolae attached to the plasma membrane of pulmonary endothelial cells present in DRM under high-fat stress.

Expression of some co-fractionated proteins (Filamin A, dynamin) with caveolin-1

Dynamin is a 96-kDa GTPase shown to be essential for many cellular processes, including the budding of endocytic (Herskovits et al. 1993) and secretor-transport (Cao et al. 2000) vesicles, podosome formation (McNiven et al. 2004), actin rearrangements (Lee and De Camilli 2002; Schafer et al. 2002) and cytokinesis (Thompson et al. 2002). This protein is also involved in the fission of some endocytic vesicles from the plasma membrane (Henley et al. 1998) and their subsequent internalization (Oh et al. 1998).

To explore whether caveolae budding from the plasma membrane was affected by the down-regulation of PTRF, we investigated, by mass spectrometry, the protein expression of dynamin in DRM. Figure 3a reveals a decrease of protein expression of dynamin in the hyperlipidemic group (~1.7-fold for the A group) comparative with physiological

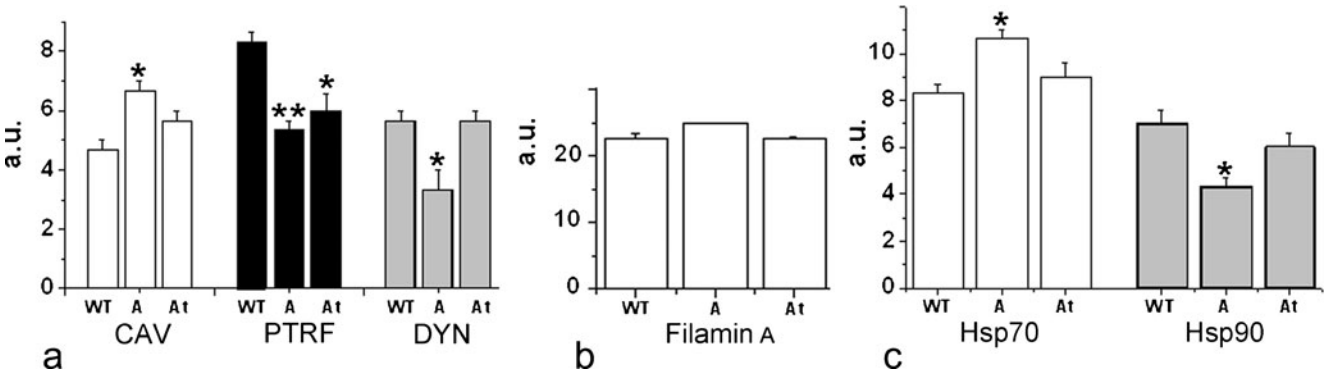

Fig. 3 Mass spectrometry proteomic analysis of DRM. Histogram showing normalized spectrum count in arbitrary units (*a.u.*; relative abundance of protein across the various samples) of (**a**) caveolin-1 (*CAV*), PTRF, dynamin (*DYN*), (**b**) Filamin A, (**c**) heat-shock proteins 70 and 90 (*Hsp70*, *Hsp90*) in DRM (fractions 4 and 5) by comparative spectral counting LC-MS/MS (liquid chromatography mass spectrometric analysis). The experiment was repeated three times. DRM were collected from each experimental group (*WT* wild-types, *A* hyperlipidemic untreated animals, *At* statin-treated animals), concentrated by ultracentrifugation and subjected to triplicate LC-MS/MS analysis. Data are expressed as means ± SEM. **P*<0.05, ***P*<0.01

conditions revealed by the WT controls. We hypothesise that the reduction in the number of caveolae attached to the plasma membrane is supported by a decreased protein expression of both PTRF and dynamin (Figs. 2e, 3a), which might be involved in the budding step of caveolae located on plasma membrane. Previously published data supporting our observations provide evidence that caveolae are associated with the cytoskeleton and other structural proteins including actin, annexin II, Filamin A and dynamin, which are thought to be important in regulating caveolae budding and transport function (Stahlhut and van Deurs 2000).

Another notable finding in our study is the Filamin A association with caveolin-1, showed by co-fractionation of these proteins in the DRM (Fig. 3b). These results correlate well with previous studies that demonstrated that Filamin A association with caveolin-1 in endothelial cells is involved in the mobility of both intracellular caveolin-1 and membrane-associated vesicles (Sverdlov et al. 2009).

Correlation of released serum Hsps and their location in DRM

The accumulation of Hsps is seen not only in stressful conditions but also in many patho-physiological conditions and tumors. These chaperones help the cell to recover by refolding partially damaged functional proteins and also by increasing the association of the cell with survival factors (Sreedhar et al. 2004). Interestingly, Hsps, which are normally located intracellularly, have also been found in soluble form in serum together with specific anti-Hsp antibodies and some data suggest a close correlation between the levels of these antibodies and the severity of atherosclerosis (Pockley et al. 1998).

Using the capture enzme-linked immunosorbent assay, we determined the concentration of secreted Hsps in hyperlipidemic serum (Table 1). With respect to the Hsp70 proteins, a real boost occurred to their secretion in the hyperlipidemic A group animals, compared with the WT and At groups. However, the Hsp90 detected in serum decreased in the A group animals compared with that of the WT group.

Statin therapy (group At) significantly reversed the processes induced by hyperlipidemia, reducing the secretion of Hsp70 while raising the secretion of Hsp90 compared with A group, together with a decline in the serum lipids (Table 1).

The co-fractionation of Hsp70 and Hsp90 (Fig. 3c) together with caveolin-1 in DRM suggests that lipid rafts and/or caveolae have a positive effect on the secretion of these Hsps. Mass spectrometry results documented that Hsp90 (Fig. 3c) was significantly lower in DRM isolated from hyperlipidemic animals (group A) compared with that in the WT group. On the contrary, Hsp70 protein expression (Fig. 3c) was found to be significantly higher in DRM isolated from the A group when compared with that of the WT group.

Mass spectrometry revealed, for the first time, the increased expression of Hsp70 protein in DRM isolated from the lung tissue of hyperlipidemic animals (Fig. 3c). The expression of Hsp70 and Hsp90 was strongly regulated in the ApoE knockout mice and these Hsps co-fractionated with caveolar and cytoskeletal proteins. An understanding of the role of Hsps in atherogenesis might help in the design of strategies that target these proteins in early diagnosis or in the treatment of disease.

Discussion

The systemic vascular dysfunction associated with atherosclerosis and the new concept of the “vulnerable patient” need to be supported by novel quantitative data and variables

to be measured. Valuable information regarding the high-lipid stress induced in vasculature, even in tissue that does not usually develop atherosclerotic plaques could allow the early assessment of high risk patients.

In this paper, we have aimed to demonstrate the effect of a high-lipid diet on biochemical changes of DRM microdomains isolated from the lung of ApoE−/− mice with atherosclerosis. Although the lung is not a target for atherosclerotic lesions, pulmonary dysfunctions and severe cardiopulmonary effects are common events associated with cardiovascular diseases. The experimental model designed by using a hyperlipidemic diet in ApoE knockout mice has demonstrated the rapid development of atherosclerotic lesions and occurrence of pathology (Fig. 1, Table 1). As previously hypothesized, the presence of a mechanism by which inflammation is maintained and enhanced under hyperlipidemic conditions leads to the development of chronic patho-physiological symptoms and, in the end, to atherosclerosis (Haraba et al. 2011). In addition, increased expression of caveolin-1, an elevated cholesterol concentration and increased ACE enzymatic activity (Figs. 2a–e, 3a) might cause the inhibition of endothelial nitric oxide synthase located on the internal face of the membrane, followed by the reduced production of nitric oxide, which ultimately leads to the dysfunction of endothelial cells. Increased cholesterol and glycerolipids in DRM induced by a high-fat diet demonstrates an enrichment of the cell membrane with lipid rafts of modified biochemical composition (Fig. 2c, d), which might significantly affect the fluidity and permeability of the cell membrane. The diet-induced changes are also supported by the high-sensitivity mass spectrometry analysis that has evidenced various pools of identified proteins in control (WT: 465±14) versus the hyperlipidemic (A: 477±6) or statin-treated group (At: 456±18).

Previously reported data have shown that PTRF expression occurs strictly in parallel to that of caveolin-1 in mice tissues, with its highest expression being found in fat and lung, predicting a functional link between the two proteins (Hasegawa et al. 2000). PTRF is recruited by caveolins to plasma membrane caveolar domains and is necessary for caveolae formation according to Liu and Pilch (2008). Indeed, the latter authors have claimed that the absence of PTRF leads to the loss of morphologically identifiable caveolae and reduced protein expression of all three caveolin isoforms, whereas no alterations at the level of mRNA of caveolins have been observed. Previous data (Hill et al. 2008) showing that PTRF down-regulation is also accompanied by an increase of caveolin-1 mobility, which is released from the cell surface and rapidly internalized and degraded, support our observations.

When a non-ionic detergent extraction such as Triton X-100 is performed and complemented by density gradient centrifugation to isolate DRM, the buoyant fractions have been shown to be a mixture of membranes from multiple organelles (Everson and Smart 2006). In our case, the hyperlipidemic diet induces changes in the DRM-associated proteins that co-fractionate with caveolin-1 as PTRF, dynamin, Hsp70 and Hsp90 and also of the major lipid components in ApoE−/− mice (Figs. 2 and 3). The low expression of PTRF is consistent with a reduced number of caveolae attached to the plasma membrane, whereas the high expression of caveolin-1 suggests the redistribution of caveolin-1 toward the non-raft domains of the cellular membranes.

Published data demonstrate that dynamin plays an essential role in receptor-mediated endocytosis via clathrin-coated pits or caveolae (Herskovits et al. 1993). In our model, a high-fat diet induces the over-expression of caveolin-1 and decreases dynamin protein expression co-fractionated with caveolin-1 in DRM. The correlated changes induced by a hyperlipidemic diet in lipids and proteins that co-fractionate with caveolin-1 (i.e., PTRF, dynamin, Filamin A) in DRM might be an indirect response of the increased internalization of macromolecules via various mechanisms and diverse dynamin-dependent pathways at the expense of the caveolar pathway in pathological conditions induced by atherosclerosis in pulmonary microvasculature (Fig. 3a, b).

Our results support the concept that membrane-associated caveolae respond to the high-lipid stress by the rapid disassembly and redistribution of caveolin-1 in non-caveolae domains at the plasma membrane level or in intracellular membranes, accompanied by the down-regulation of PTRF and dynamin protein and the up-regulation of caveolin-1 (Figs. 2e, 3a).

In addition, the data show an over-expression of Hsp70 and a down-regulation of Hsp90, both of which co-fractionate with caveolin-1 in DRM isolated from lung tissue (Fig. 3c). The cellular stress factors responsible for the induction of the Hsp70 boost in ApoE−/− mice are not known but the initial cause is likely to be lipid deposition. ApoE−/− mice lack ApoE, a glycoprotein that mediates the low-density lipoprotein (LDL) receptor clearance of serum lipoproteins (Plump and Breslow 1995) and spontaneously develop hyperlipidemia, as in humans expressing dysfunctional ApoE (Walden and Hegele 1994). Oxidized LDL in the arterial wall is chemotactic and enhances the adhesiveness of monocytes inducing the expression of Hsp60 and Hsp70 in several cell types (Johnson 1999; Frostegard et al. 1996). The present results are consistent with the concept that caveolae function as vehicles by which Hsps are transported to the cell membrane for externalization (Broquet et al. 2003). Hsp70 localized in caveolae possibly functions to prevent oxidative damage to proteins and lipids, whereas extracellular Hsp70 acts as a danger signal to the innate immune system (Vega et al. 2008).

Indeed, the hyperlipidemic condition induces a change in the distribution of Hsp70 and Hsp90 that co-fractionate with

caveolin-1 in DRM; this is correlated with the amount secreted into serum isolated from the same experimental group. These data lead us to consider the possible active regulatory role of caveolin-1-positive DRM in Hsp secretion (Fig. 3c, Table 1).

Since the present results show notable similarities with human pathology, the data obtained might be relevant to the modulation of molecular processes in patients with atherosclerosis. Future studies should investigate the cardiopulmonary effects of in vivo modulation of caveolin expression, since the accumulated data support the systemic inflammatory character of atherosclerosis.

Acknowledgments We thank Dr. Emanuel Dragan for the experimental animal models and Mrs. Maria Pascu for excellent technical assistance.

References

Bernstein KE, Xiao HD, Frenzel K, Li P, Shen XZ, Adams JW, Fuchs S (2005) Six truisms concerning ACE and the renin-angiotensin system from the genetic analysis of mice. Circ Res 96:1135–1144

Broquet AH, Thomas G, Masliah J, Trugnan G, Bachelet M (2003) Expression of the molecular chaperone Hsp70 in detergent-resistant microdomains correlates with its membrane delivery and release. J Biol Chem 278:21601–21606

Businaro R, Profumo E, Tagliani A, Buttari B, Leone S, D'Amati G, Ippoliti F, Leopizzi M, D'Arcangelo D, Capoano R, Fumagalli L, Salvati B, Riganò R (2009) Heat-shock protein 90: a novel autoantigen in human carotid atherosclerosis. Atherosclerosis 207:74–83

Cao H, Thompson HM, Krueger EW, McNiven MA (2000) Disruption of Golgi structure and function în mammalian cells expressing a mutant dynamin. J Cell Sci 113:1993–2002

Chidlow JH Jr, Sessa WC (2010) Caveolae, caveolins, and cavins: complex control of cellular signaling and inflammation. Cardiovasc Res 86:219–225

Drab M, Verkade P, Elger M, Kasper M, Lohn M, Lauterbach B, Menne J, Lindschau C, Mende F, Luft FC, Schedl A, Haller H, Kurzchalia TV (2001) Loss of caveolae, vascular dysfunction, and pulmonary defects in caveolin-1 gene-disrupted mice. Science 293:2449–2452

Durante W, Kroll MH, Christodoulides N, Peyton KJ, Schafer AI (1997) Nitric oxide induces heme oxygenase-1 gene expression and carbon monoxide production in vascular smooth muscle cells. Circ Res 80:557–564

Erman A, van Dyk DJ, Chen-Gal B, Giler ID, Rosenfeld JB, Boner G (1993) Angiotensin converting enzyme activity in the serum, lung and kidney of diabetic rats. Eur J Clin Invest 23:615–620

Everson WV, Smart EJ (2006) Caveolin and its role in intracellular chaperone complexes. In: Fielding CJ (ed) Lipid rafts and caveolae: from membrane biophysics to cell biology. Wiley-VCH, New York, pp 175–195

Frostegard J, Kjellman B, Gidlung M, Andersson B, Jindal S, Kiessling R (1996) Induction of heat shock protein in monocytic cells by oxidized low density lipoprotein. Atherosclerosis 121:93–103

Fu X, Gharib SA, Green PS, Aitken ML, Frazer DA, Park DR, Vaisar T, Heinecke JW (2008) Spectral index for assessment of differential protein expression in shotgun proteomics. J Proteome Res 7:845–854

Haraba R, Suica VI, Uyy E, Ivan L, Antohe F (2011) Hyperlipidemia stimulates the extracellular release of nuclear high mobility group box 1 protein. Cell Tissue Res 346:361–368

Hasegawa T, Takeuchi A, Miyaishi O, Xiao H, Mao J, Isobe K (2000) PTRF (polymerase I and transcript-release factor) is tissue-specific and interacts with the BFCOL1 (binding factor of a type-I collagen promoter) zinc-finger transcription factor which binds to the two mouse type-I collagen gene promoters. Biochem J 347:55–59

Henley JR, Krueger EW, Oswald BJ, McNiven MA (1998) Dynamin-mediated internalization of caveolae. J Cell Biol 141:85–99

Herskovits JS, Burgess CC, Obar RA, Vallee RB (1993) Effects of mutant rat dynamin on endocytosis. J Cell Biol 122:565–578

Hill MM, Bastiani M, Luetterforst R, Kirkham M, Kirkham A, Nixon SJ, Walser P, Abankwa D, Oorschot VM, Martin S, Hancock JF, Parton RG (2008) PTRF-cavin, a conserved cytoplasmic protein required for caveola formation and function. Cell 132:113–124

Ishihama Y, Oda Y, Tabata T, Sato T, Nagasu T, Rappsilber J, Mann M (2005) Exponentially modified protein abundance index for estimation of absolute protein amount in proteomics by the number of sequenced peptides per protein. Mol Cell Proteomics 4:1265–1272

Johnson AD (1999) Heat shock proteins in atherosclerosis. In: Latchman DS (ed) Handbook of experimental pharmacology: stress proteins. Springer, Berlin, pp 381–402

Kanwar RK, Kanwar JR, Wang D, Ormrod DJ, Krissansen GW (2001) Temporal expression of heat shock proteins 60 and 70 at lesion-prone sites during atherogenesis in ApoE-deficient mice. Arterioscler Thromb Vasc Biol 21:1991–1997

Keller A, Nesvizhskii AI, Kolker E, Aebersold R (2002) Empirical statistical model to estimate the accuracy of peptide identifications made by MS/MS and database search. Anal Chem 74:5383–5392

Kurzchalia TV, Parton RG (1996) And still they are moving dynamic properties of caveolae. FEBS Lett 389:52–54

Lee E, De Camilli P (2002) Dynamin at actin tails. Proc Natl Acad Sci U S A 99:161–166

Liu L, Pilch PF (2008) A critical role of cavin (polymerase I and transcript release factor) in caveolae formation and organization. J Biol Chem 283:4314–4322

Majkova Z, Toborek M, Hennig B (2010) The role of caveolae in endothelial cell dysfunction with a focus on nutrition and environmental toxicants. J Cell Mol Med 14:2359–2370

Mancini FP, Newland DL, Mooser V, Murata J, Marcovina S, Young SG, Hammer RE, Sanan DA, Hobbs HH (1995) Relative contributions of apolipoprotein A and apolipoprotein B to the development of fatty lesions in the proximal aorta of mice. Arterioscler Thromb Vasc Biol 15:1911–1916

McNiven MA, Baldassarre M, Buccione R (2004) The role of dynamin în the assembly and function of podosomes and invadopodia. Front Biosci 9:1944–1953

Mehta TA, Greenman J, Ettelaie C, Venkatasubramaniam A, Chetter IC, McCollum PT (2005) Heat shock proteins in vascular disease. Eur J Vasc Endovasc Surg 29:395–402

Muzykantov VR, Danilov SM (1991) New approaches to investigations of oxidative injury to the pulmonary endothelium: a minireview. Biomed Sci 2:11–22

Nabi IR (2009) Cavin fever: regulating caveolae. Nat Cell Biol 11:789–791

Naghavi M, Libby P, Falk E, Casscells SW, Litovsky S, Rumberger J et al (2003) From vulnerable plaque to vulnerable patient: a call for a new definitions and risk assessement strategies: part I. Circulation 108:1664–1672

Nakamura K, Sasaki T, Cheng XW, Iguchi A, Sato K, Kuzuya M (2009) Statin prevents plaque disruption in apoE-knockout mouse model through pleiotropic effect on acute inflammation. Atherosclerosis 206:355–361

Nakashima Y, Plump AS, Raines EW, Breslow JL, Ross R (1994) ApoE deficient mice develop lesions of all phases of atherosclerosis throughout the arterial tree. Arterioscler Thromb 14:133–140

Nesvizhskii AI, Keller A, Kolker E, Aebersold R (2003) A statistical model for identifying proteins by tandem mass spectrometry. Anal Chem 75:4646–4658

Nollen EA, Morimoto RI (2002) Chaperoning signaling pathways: molecular chaperones as stress-sensing "heat shock"' proteins. J Cell Sci 115:2809–2816

Oh P, McIntosh DP, Schnitzer JE (1998) Dynamin at the neck of caveolae mediates their budding to form transport vesicles by GTP-driven fission from the plasma membrane of endothelium. J Cell Biol 141:101–114

Orfanos SE, Armaganidis A, Glynos C, Psevdi E, Kaltsas P, Sarafidou P, Catravas JD, Dafni UG, Langleben D, Roussos C (2000) Pulmonary capillary endothelium-bound angiotensin-converting enzyme activity in acute lung injury. Circulation 102:2011–2018

Plump AS, Breslow JL (1995) Apolipoprotein E and the apolipoprotein E-deficient mouse. Annu Rev Nutr 15:495–518

Pockley AG (2002) Heat shock proteins, inflammation, and cardiovascular disease. Circulation 105:1012–1017

Pockley AG, Frostegard J (2005) Heat shock proteins in cardiovascular disease and the prognostic value of heat shock protein related measurements. Heart 91:1124–1126

Pockley AG, Shepherd J, Corton JM (1998) Detection of heat shock protein 70 (Hsp70) and anti-Hsp70 antibodies in the serum of normal individuals. Immunol Invest 27:367–377

Pratt WB, Toft DO (2003) Regulation of signaling protein function and trafficking by the Hsp90/Hsp70-based chaperone machinery. Exp Biol Med 228:111–133

Razani B, Lisanti MP (2001) Caveolins and caveolae: molecular and functional relationships. Exp Cell Res 271:36–44

Rizzo V, Sung A, Oh P, Schnitzer JE (1998) Rapid mechanotransduction in situ at the luminal cell surface of vascular endothelium and its caveolae. J Biol Chem 273:26323–26329

Sargiacomo M, Sudol M, Tang ZL, Lisanti MP (1993) Signal transducing molecules and GPI-linked proteins form a caveolin-rich insoluble complex in MDCK cells. J Cell Biol 122:789–807

Schafer DA, Weed SA, Binns D, Karginov AV, Parsons JT, Cooper JA (2002) Dynamin 2 and cortactin regulate actin assembly and filament organization. Curr Biol 12:1852–1857

Simionescu M, Antohe F (2006) Functional ultrastructure of the vascular endothelium—changes in various pathologies. In: Moncada S, Higgs A (eds) Handbook of physiology and bichemistry, vol 176/I. Springer, Berlin, pp 41–69

Simionescu M, Simionescu N (1991) Endothelial transport of macromolecules: transcytosis and endocytosis. Cell Biol Rev 25:1–80

Smith JD, Breslow JL (1997) The emergence of mouse models of atherosclerosis and their relevance to clinical research. J Intern Med 242:99–109

Sreedhar AS, Soti C, Csermely P (2004) Inhibition of Hsp90: a new strategy for inhibiting protein kinases. Biochim Biophys Acta 1697:233–242

Stahlhut M, Deurs B van (2000) Identification of Filamin as a novel ligand for caveolin-1: evidence for the organization of caveolin-associated membrane domains by the actin cytoskeleton. Mol Biol Cell 11:325–337

Sverdlov M, Shinin V, Place AT, Castellon M, Minshall RD (2009) Filamin A regulates caveolae internalization and trafficking in endothelial cells. Mol Biol Cell 20:4531–4540

Thompson HM, Skop AR, Euteneuer U, Meyer BJ, McNiven MA (2002) The large GTPase dynamin associates with the spindle midzone and is required for cytokinesis. Curr Biol 12:2111–2117

Tsan MF, Gao B (2004) Heat shock protein and innate immunity. Cell Mol Immunol 1:274–279

Uyy E, Antohe F, Ivan L, Haraba R, Radu DL, Simionescu M (2010) Upregulation of caveolin-1 expression is associated with structural modifications of endothelial cells in diabetic lung. Microvasc Res 79:154–159

Vega VL, Rodríguez-Silva M, Frey T, Gehrmann M, Diaz JC, Steinem C, Multhoff G, Arispe N, De Maio A (2008) Hsp70 translocates into the plasma membrane after stress and is released into the extracellular environment in a membrane-associated form that activates macrophages. J Immunol 180:4299–4307

Walden CC, Hegele RA (1994) Apolipoprotein E in hyperlipidemia. Ann Intern Med 120:1026–1036

Wick G (2006) The heat is on: heat-shock proteins and atherosclerosis. Circulation 114:870–872

Wick G, Knoflach M, Xu Q (2004) Autoimmune and inflammatory mechanisms in atherosclerosis. Annu Rev Immunol 22:361–403

Zhang SH, Reddick RL, Piedrahita JA, Maeda N (1992) Spontaneous hypercholesterolemia and arterial lesions in mice lacking apolipoprotein E. Science 258:468–471